water

MDPI

Article

Investigating Climate Change Effects on Evapotranspiration and Groundwater Recharge of the Nile Delta Aquifer, Egypt

Mohamed Galal Eltarabily [1,2], Ismail Abd-Elaty [3], Ahmed Elbeltagi [4], Martina Zeleňáková [5,*] and Ismail Fathy [3]

[1] Department of Land, Air and Water Resources, University of California, Davis, CA 95616, USA
[2] Civil Engineering Department, Faculty of Engineering, Port Said University, Port Said 42523, Egypt
[3] Department of Water and Water Structures Engineering, Faculty of Engineering, Zagazig University, Zagazig 44519, Egypt
[4] Agricultural Engineering Department, Faculty of Agriculture, Mansoura University, Mansoura 35516, Egypt
[5] Civil Engineering Department, University for Business and Technology, 10000 Pristina, Kosovo
* Correspondence: martina.zelenakova@tuke.sk; Tel.: +383-55-602-4270

Abstract: Climate change (CC) directly affects crops' growth stages or level of maturity, solar radiation, humidity, temperature, and wind speed, and thus crop evapotranspiration (ET_c). Increased crop ET_c shifts the fraction of discharge from groundwater aquifers, while long-term shifts in discharge can change the groundwater level and, subsequently, aquifer storage. The long-term effect of CC on the groundwater flow under different values of ET_c was assessed for the Nile Delta aquifer (NDA) in Egypt. To quantify such impacts, numerical modeling using MODFLOW was set up to simulate the groundwater flow and differences in groundwater levels in the long term in the years 2030, 2050, and 2070. The model was initially calibrated against the hydraulic conductivity of the aquifer layers of the groundwater levels in the year 2008 from 60 observation wells throughout the study area. Then, it was validated with the current groundwater levels using an independent set of data (23 points), obtaining a very good agreement between the calculated and observed heads. The results showed that the combination of solar radiation, vapor pressure deficit, and humidity (H) are the best variables for predicting ET_c in Nile Delta zones (north, middle, and south). ET_c among the whole Nile Delta will increase by 11.2, 15.0, and 19.0% for the years 2030, 2050, and 2070, respectively. Zone budget analysis revealed that the increase of ET_c will decrease the inflow and the groundwater head difference (GWHD). Recharge of the aquifer will be decreased by 19.74, 27.16, and 36.84% in 2030, 2050, and 2070, respectively. The GWHD will record 0.95 m, 1.05 m, and 1.40 m in 2030, 2050, and 2070, respectively when considering the increase of ET_c. This reduction will lead to a slight decline in the storage of the Nile Delta groundwater aquifer. Our findings support the decision of the designers and the policymakers to guarantee a long-term sustainable management plan of the groundwater for the NDA and deltas with similar climate conditions.

Keywords: climate change; evapotranspiration; linear regression; MODFLOW; Nile Delta

Citation: Eltarabily, M.G.; Abd-Elaty, I.; Elbeltagi, A.; Zeleňáková, M.; Fathy, I. Investigating Climate Change Effects on Evapotranspiration and Groundwater Recharge of the Nile Delta Aquifer, Egypt. *Water* **2023**, *15*, 572. https://doi.org/10.3390/w15030572

Academic Editor: Aizhong Ye

Received: 28 December 2022
Revised: 20 January 2023
Accepted: 29 January 2023
Published: 1 February 2023

1. Introduction

Water resources are one of the most important natural resources worldwide [1,2]; sustainable management plans are essential for ensuring the long-term availability of these sources, especially in arid and semi-arid regions [3–6]. The agriculture sector is the highest water consumer. Therefore, successful irrigation management practices should consider the rational use of water alongside the maximum water use efficiency, high yield of crops, and return profit [7–9]. The source of irrigation water can be surface water or groundwater. The quality of irrigation water should be considered when looking for sustainable agricultural practices [10]. Knowing exactly how much water is needed to fulfill crop requirements helps growers to utilize the irrigation water more efficiently with minimal deterioration to water sources [11]. Thus, the accurate estimation of crop evapotranspiration (ET_c) is

crucial for the operation and designing of irrigation systems, irrigation scheduling, and entire management plans of irrigation water [12].

Evapotranspiration is a process governed by the energy and heat exchanges at the land surface, which is controlled by the amount of available energy on the ground [13]. Additionally, it reflects the crop water requirements during the growing season and how much water is required for plants [14]. The estimation of spatially distributed crop water consumption is challenging but important to determine water balance at different scales to promote the efficient management of water resources [15]. Additionally, ET_c from irrigated agriculture (e.g., the case of the Nile Delta of Egypt) is an important concern in arid and semi-arid regions, where it has a substantial impact on groundwater resource depletion and water management plans [16,17].

Moreover, ET_c employs a key role in the watershed budget analysis [18], and a wide range of techniques have been developed to precisely estimate its spatial and temporal variability at site-specific locations. Moreover, it is generally considered in the hydrological modeling of surface water [19] by integrating empirical formulas, such as the Penman–Monteith equation [20], based on climate variables including temperature, solar radiation, wind speed, and humidity. The estimation of ET_c is most important in the hydrological modeling of surface water, where it is not directly included in groundwater modeling [21]. ET_c is neglected in groundwater modeling when aquifers are formed by coarse-grained sediments where the capillary rise is very low [22]. For leaky aquifers such as the NDA, ET_c must be considered by subtracting from precipitation and irrigation water to calculate the input recharge to the groundwater flow models [23], especially when the water table is relatively shallow [24].

There are several ways to calculate the actual ET_c, but surface energy balance methods [25] and surface water balance methods [25,26] are mainly used. Rana and Katerji [27] provided a summary of 10 methods for measuring and calculating actual ET_c. The approaches were classified as hydrological, micrometeorological, and plant-physiological, depending on their use. Every approach has advantages and disadvantages. Xu and Chen [28] showed that a weighted lysimeter, for example, can offer precise information on water balance; nevertheless, it is difficult to estimate the ET_c across large regions for an extended length of time. As a result, actual ET_c is typically calculated using less sophisticated physically based or empirical methods. According to Linacre [29], actual ET_c may be estimated using a link between accessible soil water content and evaporation rate. Actual ET_c was estimated using two methods: the first method is the ET_c model developed by Han and Tian [30], and the second method is the soil water balance model, in which the actual ET_c is estimated by the fraction of potential ET_c; this fraction increases as soil water content increases.

Egypt faces several serious risks from CC, and the Nile Delta (ND) is now seriously suffering from these risks, such as rising sea level, saltwater intrusion, salinization, higher temperatures, and land subsidence [31]. The impacts of these effects on surface water and groundwater should be carefully addressed and the adaptation scenarios for mitigation must be prepared [32,33]. The agriculture sector has been negatively influenced by higher temperatures for lower crop productivity and the loss of some agricultural lands in the ND [34], where the productivity of crops was estimated to decrease by 1 to 17%. Moreover, climatic changes have economic and environmental impacts which should be considered to ensure food security [35].

The groundwater recharge in the NDA is mainly sourced from irrigation water, inflow from the two branches of the Nile River, Damietta and Rosetta, and rainfall along the northern coast [36]. Groundwater recharge depends on the rainfall duration and intensity, evapotranspiration rates, infiltration rates, soil moisture, aquifer permeability, and groundwater table depths [37]. Moreover, ET_c and soil moisture depletion depend on climatic parameters such as temperature, relative humidity, wind speed, and sunshine hours. The climatic parameters should be considered for estimating the ET_c and soil moisture depletion pattern to investigate the influence of CC on groundwater recharge [38].

While flood irrigation is traditionally practiced in the ND of Egypt and the return flow from irrigation water is the main component of groundwater recharge for the NDA, accurate predicting of ET_c is essential to quantify how much water will recharge the aquifer in the long term when the same irrigation method is still applied.

To date, there has been no accurate estimation of actual ET_c where assumptions and uncertainty of CC patterns exist. Based on the hydrological cycle, Milly and Dunne [39] determined that the actual ET_c over the Mississippi River basin increased between 1949 and 1997 due to higher precipitation and increasing water usage. Golubev et al. [40] discovered that the actual ET_c increased in certain relatively dry sections of southern Russia and Ohio over the warm seasons of 1950–1990 using large weighted lysimeters, whereas actual evaporation decreased in two wetter taiga areas. Similarly, Linacre [29] observed that decreased pan evaporation did not always imply declining actual ET_c. Trends for potential ET_c during the last 50 years in the ND have been established recently [41–44], but a predictive trend of actual ET_c has not been included in the ND aquifer modeling. Thus, our novel approach is to incorporate "near to accurate" predictive values of ET_c into the numerical simulation model of the groundwater in the ND of Egypt. The objective of this study is therefore to investigate the effect of climate change on annual actual ET_c throughout three zones of the ND (north, middle, and south) based on the historical data from 1958 to 2020 for predicting groundwater flow and differences in groundwater heads, and aquifer storage for the years 2030, 2050, and 2070. Our findings support the sustainable management plans of groundwater in the ND of Egypt for guaranteeing the sustainable use of water resources.

2. Materials and Methods

2.1. The Nile Delta Study Area

The Nile Delta (ND) of Egypt is located between the latitudes 30°00′ and 31°45′ N and longitudes 29°30′ and 32°30′ E (Figure 1a). This area is bounded by the Mediterranean Sea in the north and Ismailia and Nubaria canals in the east and west, respectively. The direction of the ground surface slopes is from the south to the north (the Mediterranean Sea) [45]. The average range of the daily temperature is between 17 °C to 20 °C [46], while the average rainfall is between 250 mm year^{-1} in the north to 200 mm year^{-1} in the south and middle parts of the ND [47]. Additionally, the evaporation rates range between 7 mm day^{-1} in Upper Egypt to about 4 mm day^{-1} on the Northern Mediterranean coast [48]. Figure 1b shows the hydrological cross-section from south to north along the ND aquifer where the hydraulic conductivity is in m day^{-1}. Figure 1c shows the land use and land cover for the ND in 2015 which was used as a base map for assigning ET_c in the model simulation. Only the temporal variation of ET_c was considered in the simulation, while the spatial variation of ET_c was not included where the land use/land (LU/LC) cover in the year 2015 (LU/LC) was assumed to be almost the same during the simulation period. This is because a precise prediction of LU/LC maps requires detecting and analyzing the changes in LU/LC satellite high-resolution images over an adequate period, which was not our main objective.

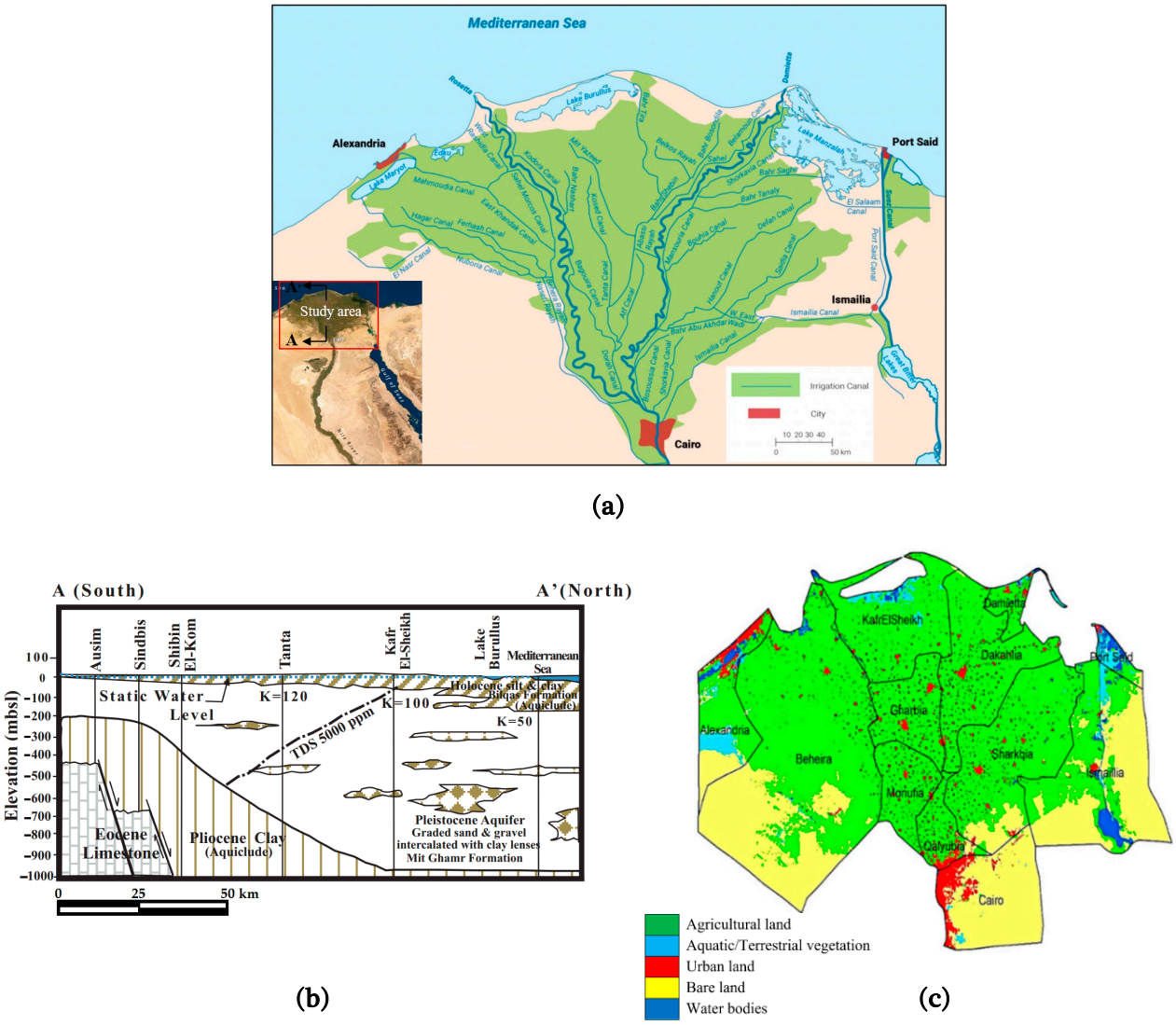

Figure 1. (**a**) Key map of the Nile Delta. (**b**) Hydrogeological cross-section from south to north along the Nile Delta aquifer [49]. (**c**) The major five land use/land cover classes in the Nile Delta in 2015 [50].

The Nile Delta aquifer (NDA) is a semi-confined aquifer that is covered by a clay cap. The thickness of clay ranges from 5 m in the south to 20 m in the middle, reaching 50 m in the North of the ND [51–53]. Said [54] illustrated that the stratigraphic of the quaternary sediments is divided into two units: the first unit is the Holocene deposits, formed by silty and sandy clay, and the second is the Pleistocene deposits, which represent the main aquifer. The average thickness of the NDA is about 200 m on the south to 900 m on the north. The hydraulic conductivity of the NDA ranges between 50 m day^{-1} to 120 m day^{-1} [55]. The aquifer transmissivity ranges between 2000 m^2 day^{-1} to 3000 m^2 day^{-1}, and the effective and total porosity ranges between 12% to 40% [56]. According to Morsy [57] and Abd-Elhamid et al. [58], the average depth of the groundwater levels ranges from 3 m to 5 m, while the groundwater flow direction is from the southeast to the northwest (Figure 2).

The NDA recharge rates, groundwater heads, flow directions, thickness of clay cap, and hydraulic conductivities are controlled and managed by the distribution and the flow of the surface water system [59,60]. This aquifer is recharged by infiltration from rainfall, surface water, and excess irrigation water. The total groundwater abstractions from the NDA are 85% of the groundwater resources in Egypt [61–63].

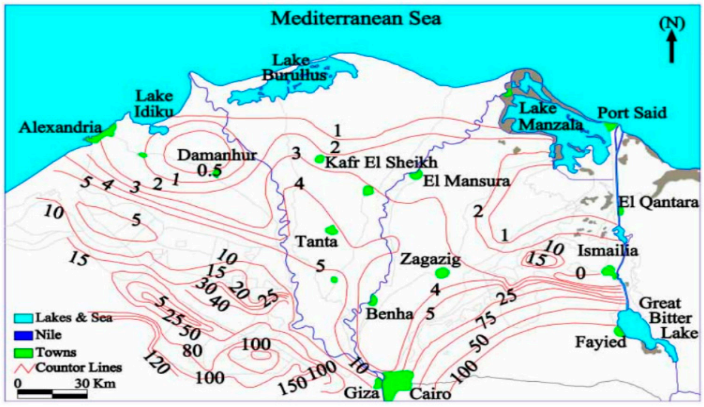

Figure 2. Average depth of groundwater in m [57,64].

2.2. Crop Consumptions

Crop water requirements are the major component of the water balance in the ND. Thus, updating the crop requirements is essential and important when considering all agroclimatic zones, climatic-dependent ET_c, and crop coefficients [65]. Figure 3 shows the yearly averaged values of the actual ET_c (in cm) for the three zones of the ND, according to the finding of "The National Commission on Water Requirements" using the Penman–Monteith equation based on the monthly meteorological data. Actual ET_c was calculated based on the crop water requirements for maize and wheat, which were selected as two major crops for this study area. This is because wheat is the most important food security crop and is the major winter cereal grain crop, while maize is the second most important grain crop according to the Food and Agricultural Organization [66]. Additionally, Egypt is currently cultivating the largest area of wheat in its history at 3.6 million acres, which is equivalent to a third of Egypt's agricultural area. Maize is grown and harvested principally in summer from May to October, while wheat is grown in the winter season. ET_c increased from 1958 to 1964 and decreased from 1964 to 1981. Additionally, it increased in the year 1982 and returned to decreasing from 1982 to 1999, while it increased in the year 2000. From 2000 to 2007, it decreased, returning to an increase from 2007 to 2020. This cycling behavior of the ET_c can be observed over the years studied (Figure 3), which is attributed to the variation of these climate variables and climate change.

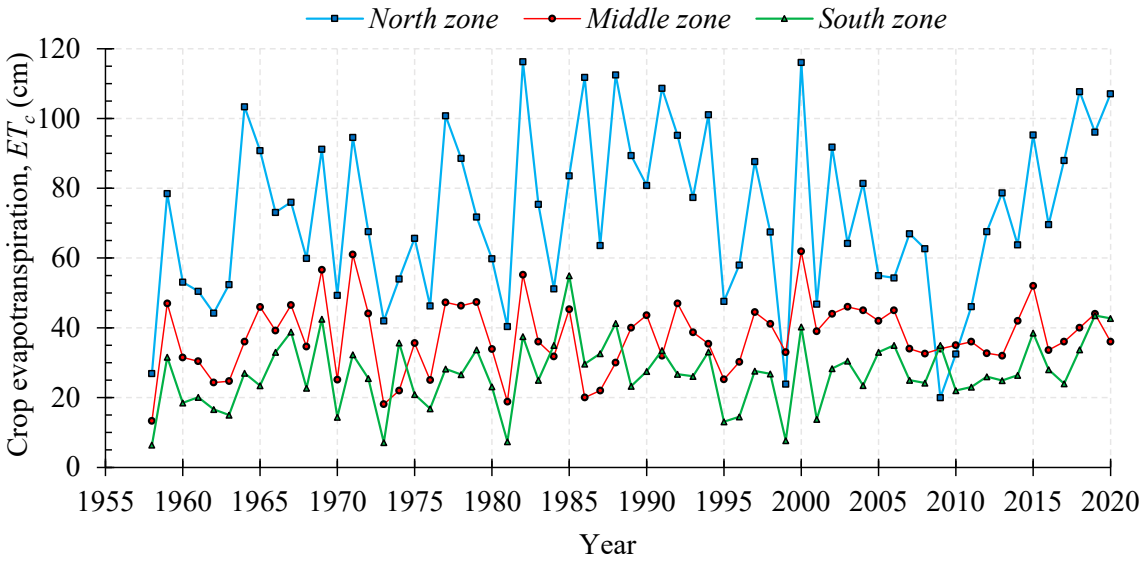

Figure 3. Historical data between 1958 and 2020 for the average ET_c (cm) for the three zones of the Nile delta in the previous 62 years.

2.3. Data Collection

Environmental Systems Research Institute (ESRI) Arc GIS software 10.2.2 was used to extract the monthly minimum temperature (T_{min}), mean temperature (T_{mean}), maximum temperature (T_{max}), wind speed (WS), solar radiation (SR), humidity (H), and precipitation (rainfall, P) from the open access data, with a geographical resolution of around 4 km^2. Temperature data were collected from the Climatic Research Unit (CRU) Time-Series (Ts) 4.0 in Network Common Data Format (NetCDF) format at 0.5° grid for the global land surface [67]. The Japanese Reanalysis (JRA-55) was used to collect the solar radiation, wind speed, and vapor pressure deficit data in NetCDF format as well [68]. The JRA-55 provided complete spatio-temporal data covering the period from 1958 to the present [69]. Additionally, World Weather Online (https://www.worldweatheronline.com/eg.aspx (accessed on 1 August 2022) was used to collect the humidity data. These datasets have been used in previous research of modeling the long-term dynamics of crop ET_c and the impact of CC on the water footprint in the ND using an artificial neural network [69], using deep learning [70], using a deep neural network [71], and using Gaussian process regression [72].

2.4. Model Description

The groundwater modeling system (GMS) was applied and used to develop the required 3D simulation model in the current study area. The MODFLOW is a modular, three-dimensional finite-difference groundwater flow model. The governing flow equation based on water balance [73] is written as follows:

$$\frac{\partial}{\partial x}\left(K_x \frac{\partial h}{\partial x}\right) + \frac{\partial}{\partial y}\left(K_y \frac{\partial h}{\partial y}\right) + \frac{\partial}{\partial z}\left(K_Z \frac{\partial h}{\partial z}\right) = S_s \frac{\partial h}{\partial t} + q_s \text{ Eqn.} \quad (1)$$

where K_x, K_y, and K_z are the hydraulic conductivities along the x, y, and z directions (LT^{-1}), respectively, h is the piezometric head (L), q_s is the volumetric flux per unit volume at sources or sinks in the porous medium (T^{-1}), S_s is the specific storage of the porous medium (L^{-1}), and t is time (T). Figure 4a shows the model grid and boundary conditions used in the simulation, while Figure 4b,c show a vertical and horizontal cross-section along the conceptual model.

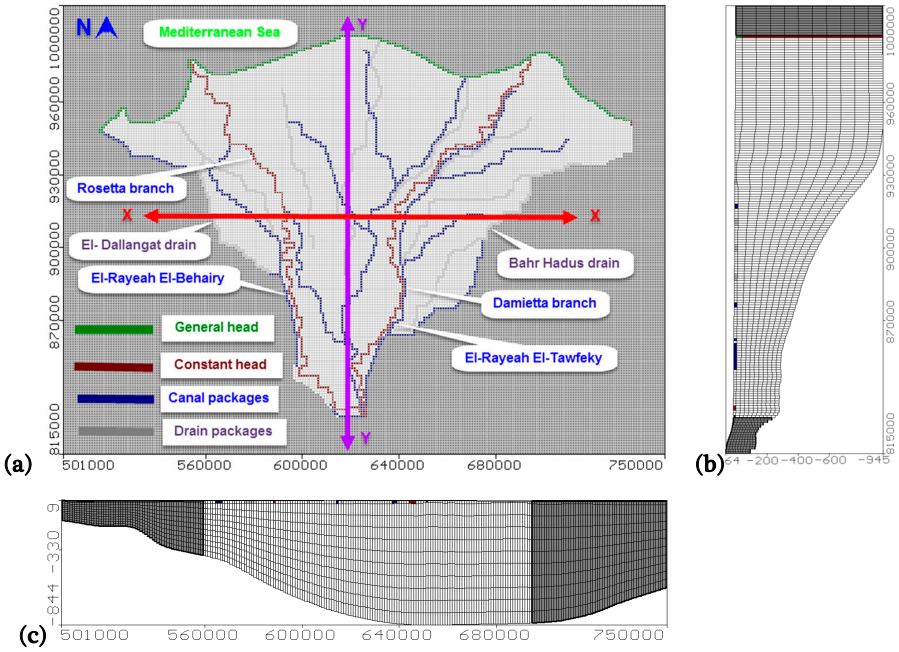

Figure 4. (**a**) Model grid and boundary conditions; (**b**) hydrogeological vertical cross-section; (**c**) hydrogeological horizontal cross-section of the underlying aquifer assigned in the simulation.

Model Calibration

The groundwater flow model was calibrated using 60 field observation wells during the year 2008 [57]. The model was calibrated for steady-state conditions using the initial hydraulic parameters presented in Table 1 by trial and error until simulated groundwater levels matched those measured in the 60 observation wells. After model calibration, the groundwater flow model was validated with an independent set of data (23 points). The residuals between the simulated and the observed groundwater heads ranged from −0.834 to 0.01 m. The absolute mean residual was 0.277 m, while the root mean squared error (RMSE) was 0.354 m, with a normalization RMSE of 2.72% (Figure 5a). This relative agreement of parameters suggests a good correlation between simulated groundwater levels (Figure 5b). The locations of the observation wells used for model calibration and validation are shown in Figure 5c. The results of the groundwater levels in the NDA ranged from 14 m to 0 m above mean sea level (MSL) (Figure 5d); additionally, the groundwater flowed from the South to the North.

Table 1. Initial and calibrated hydraulic parameters of the two geologic units of the Nile Delta aquifer.

Case	Unit	Layer No.	Horizontal and Vertical Hydraulic Conductivities		Specific Storage Ss (m^{-1})	Specific Yield Sy (-)	Effective Porosity (%)	Recharge (mm day^{-1})
			K_h (m day^{-1})	K_v (m day^{-1})				
Initial	Clay cap	1	0.10–0.25	0.01–0.025	10^{-3}	0.10	50–60	0.25–0.80
	Quaternary aquifer	2–11	5–100	0.50–10	5×10^{-3}–5×10^{-4}	0.15–0.20	30–20	
Calibrated	Clay cap	1	0.35	0.035	10^{-3}	0.10	50–60	0.01–1.05
	Quaternary aquifer	2–11	25–150	2.5–15	5×10^{-3}–5×10^{-4}	0.15–0.20	30–20	

2.5. Climate Trend Analysis

Fundamentally, trend analysis is a strategy for understanding how and why things have changed—or will change—over time. One thing to keep in mind while seeking to comprehend trend analysis is the vast range of disciplinary contexts in which it is addressed. This makes it more difficult to describe universally, but for the sake of clarity, it may be defined here as a technique for analysis that collects data and then seeks to uncover patterns, or trends, within that data to explain or anticipate behaviors. A statistical study of trends inside time-series datasets would allow for direct conclusions on existing trends or patterns within the datasets, as well as future projections (e.g., population growth or decline). These fundamental ideas have been used in a variety of statistical trend studies in the past and continue to be relevant in scenario-building exercises and future research. The statistical methods employed in such studies vary, and there are no "automatic" trend analysis procedures that can supply all of the answers, such as reference evapotranspiration [74,75], evaporation [39], and actual ET_c [76]. Therefore, trend analysis is imperfect in certain ways, but it can help analysts to recognize patterns and trends that would not be feasible otherwise. Many statistical approaches, such as the Bayesian process, Spearman's Rho test, Mann–Kendall test, and Sen's slope estimator, have been developed to find trends within time series. In this study, to detect actual ET_c trends, one parametric approach (linear regression) was used.

2.6. Case Scenarios

The MODFLOW simulated the groundwater flow and predicted the water heads for three projected periods, including the years 2030, 2050, and 2070, considering the impact of changing ET_c as a discharge component of the out-flow budget of the groundwater aquifer. These simulation procedures allow a long-term assessment of the NDA behavior and the storage potential for the increasing pattern of temperature.

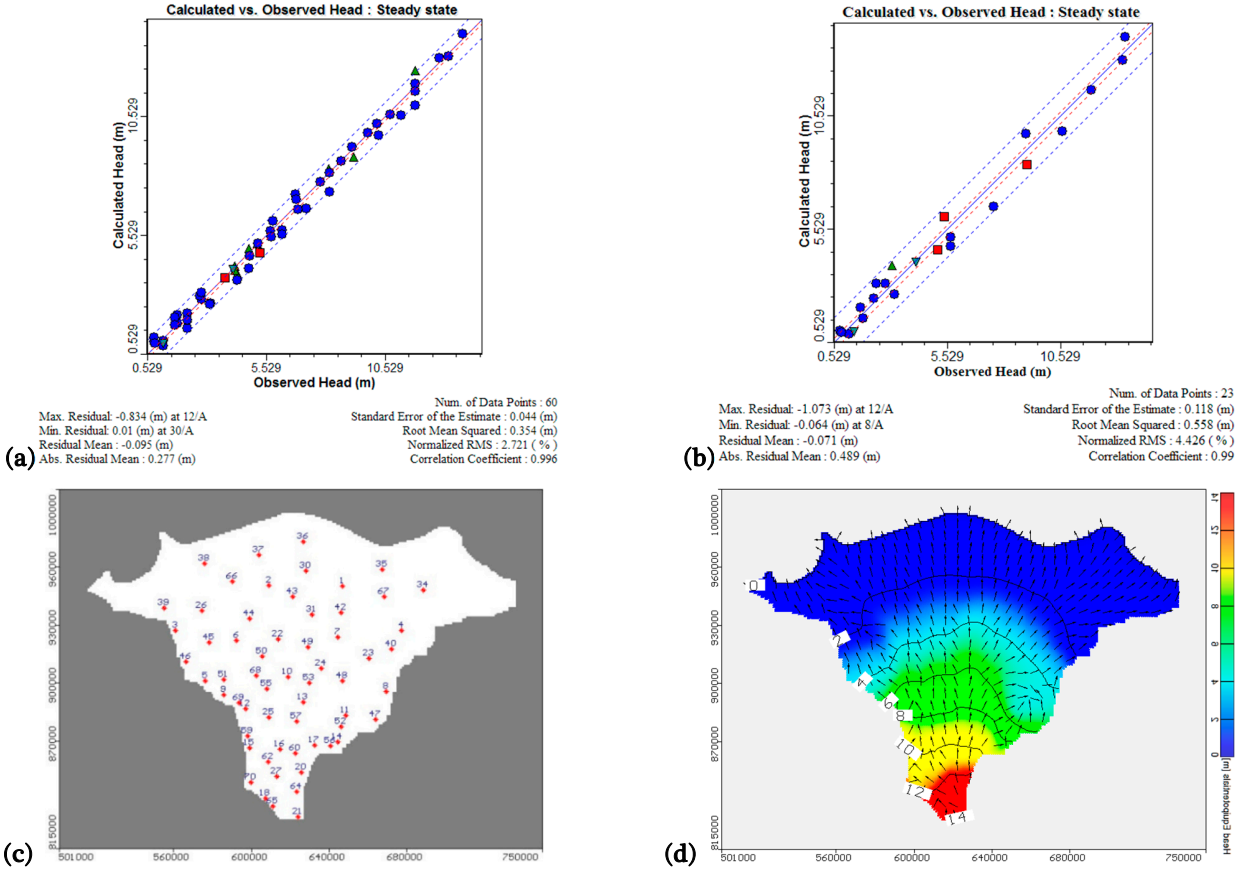

Figure 5. Observed vs. calculated groundwater heads (m) in steady-state condition for (**a**) model calibration; (**b**) model validation (solid line represents the 45° line while the red and blue dotted lines represent the error bounds of ± 5% and ± 10%, respectively; (**c**) location of the observation wells used for model calibration and validation; (**d**) groundwater head distributions for the Nile Delta Quaternary aquifer (contour lines are in black while arrows represent velocity vectors).

3. Results and Discussion

3.1. Trend Analysis of Actual Evapotranspiration in the Nile Delta

Results of the trend analysis for the annual actual ET_c series over 1958–2020 are shown in Figure 6a–c for the three zones in the study area. The mean, median, and mode of the historical data from 1958 to 2020 for the north zone of the ND were 72.13, 69.6, and 67.6, respectively. They recorded 37.28, 36, and 36 for the middle zone, and 27.06, 26.7, and 35 for the southern zone of the ND. The analysis showed increases in annual values of actual ET_c in the three zones. Increased actual ET_c was due to increasing values of climate parameters. The combination of solar radiation, vapor pressure deficit, and humidity (H) were found to be the best variables for predicting ET_c. The increasing percentages were 16.26, 8.76, and 12.31% for the northern zone, middle zone, and southern zone of the ND, respectively.

Furthermore, Figure 7 shows the future linear projections for actual ET_c in comparison with historical time series. In the North zone of the ND, the actual ET_c will reach 78.80, 82.05, and 85.30 cm year^{-1} in the years 2030, 2050, and 2070, respectively, compared with 72.13 cm year^{-1}. This represents an increase of 9.25, 12.59, and 16.05% in crop ET_c in 2030, 2050, and 2070, respectively. ET_c at the middle zone of the ND will reach 40.87, 42.62, and 44.37 cm year^{-1} compared with 37.28 cm year^{-1}, with an increase of 9.63, 13.07, and 16.65%, respectively, for the years 2030, 2050, and 2070, respectively. In addition, the actual ET_c for the southern zone will increase to 32.10, 34.56, and 37.03 cm year^{-1} compared with 27.06 cm year^{-1} which equals 18.65, 23.38, and 28.84% increase that the ET_c values between 1958 and 2020. The average value of actual ET_c among the whole ND will reach 50.60, 53.08, and 55.57 cm year^{-1} compared with 45.49 cm year^{-1}, with an increase of 11.2, 15.0, and

19.0% for the years 2030, 2050, and 2070, respectively. These values of ET_c were used as the mean ET_c rate and applied to the whole NDA when running MODFLOW to simulate the groundwater modeling, and in order to determine the decline in groundwater levels by the years 2030, 2050, and 2070.

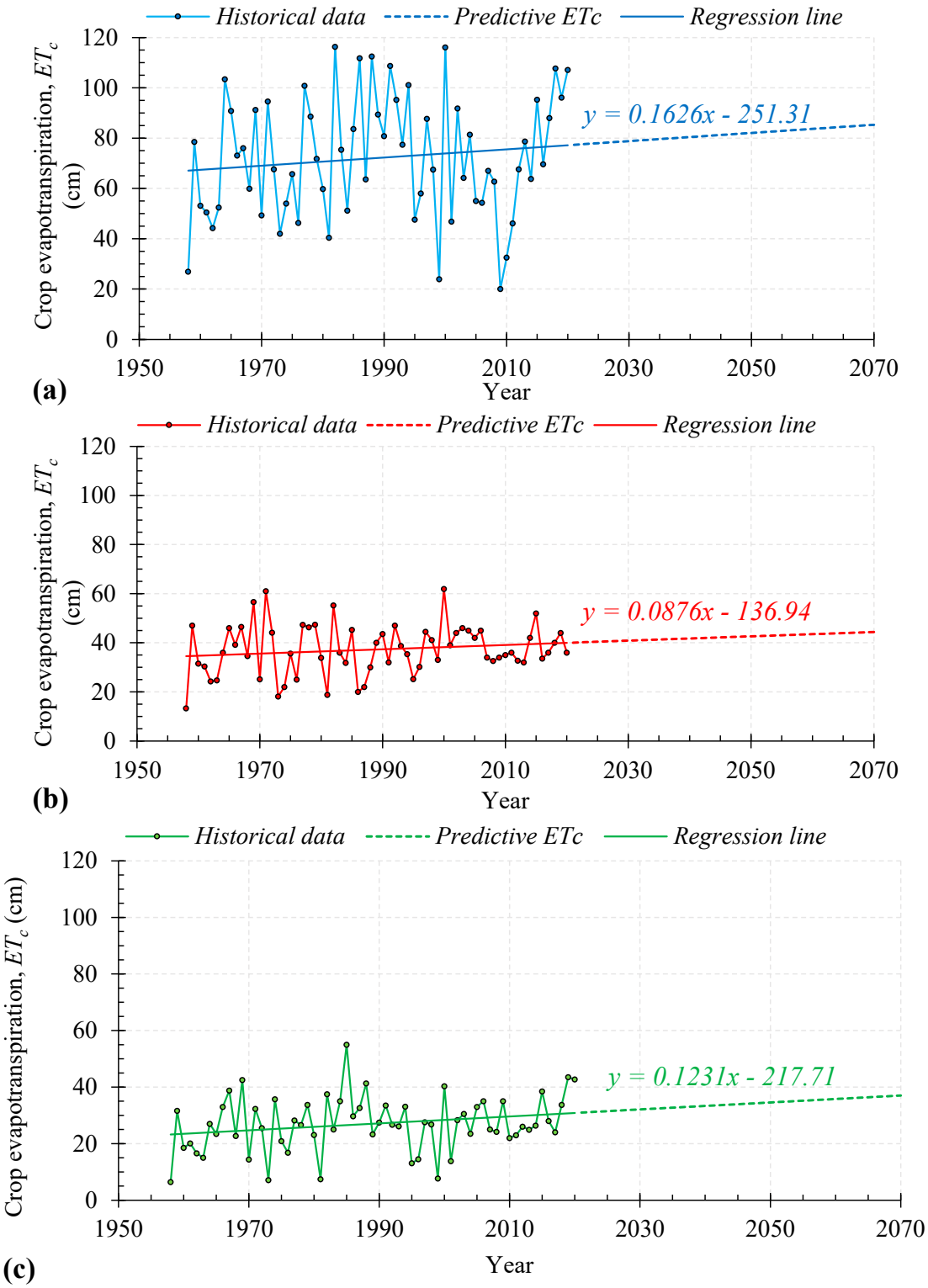

Figure 6. Trend analysis of actual evapotranspiration for historical data from 1958 to 2020, and the linear regression for the predictive values until 2070 for the three zones of the Nile Delta: (**a**) North, (**b**) Middle, and (**c**) South.

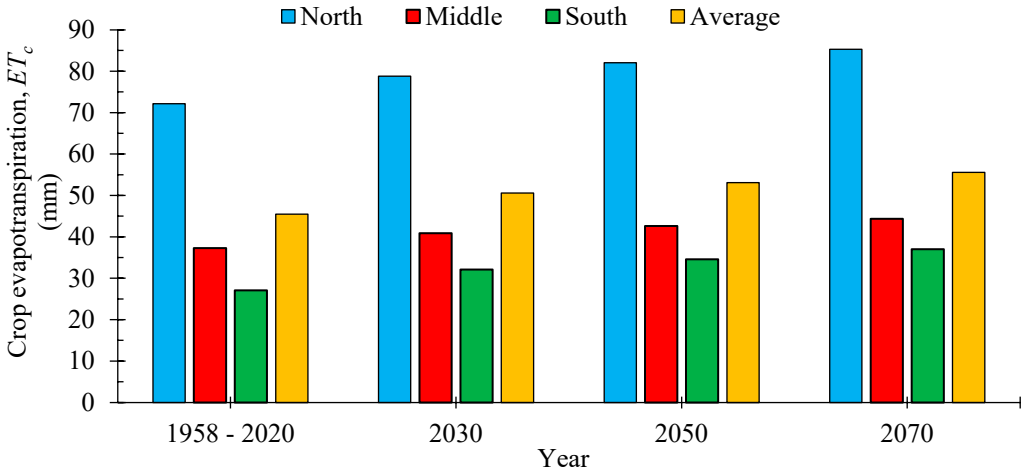

Figure 7. Future projection of actual *ET* compared with the historical period.

3.2. Hydrological Water Balance of Nile Delta Aquifer

The calibrated model was applied to simulate the future changes of ET_c and its impact on the groundwater levels in the ND for the years 2030, 2050, and 2070. Table 2 presents the zone budget analysis for the three predefined predictive periods in which the constant heads inflow was increased to 1,073,700, 1,102,500, and 1,208,900 m^3 day^{-1} compared with 840,030 m^3 day^{-1} at base case (2008); additionally, the aquifer recharge was decreased to 4,815,900, 4,692,300, and 4,271,700 m^3 day^{-1} compared with 840,030 m^3 day^{-1} at base case, while the canal leakage increased to 985,600, 1,014,400 and 1,116,100 m^3 day^{-1} compared with 732,910 m^3 day^{-1} for the base case.

Table 2. Zone budget analysis for the base case (at 2020), 2030, 2050, and 2070 (values in m^3 day^{-1}).

Boundary Parameter	Base Case	Simulation Period		
		Until 2030	Until 2050	Until 2070
Constant heads	840,030	1,073,700	1,102,500	1,208,900
Flow into the aquifer	6,000,400	4,815,900	4,692,300	4,271,700
Canals leakage	732,910	985,600	1,014,400	1,116,100
Total inflow	7,573,340	6,875,200	6,809,200	6,596,700
Constant heads	1,656,200	1,394,600	1,370,400	1,292,200
Wells	4,378,700	4,378,700	4,378,700	4,378,700
Drains	1,480,900	1,068,100	1,027,700	897,500
Canal leakage	23,176	6,167.40	5,572.80	3,888.50
General heads	34,346	27,614	26,913	24,522
Total outflow	7,573,322	6,875,181	6,809,286	6,596,811

Thus, the outflow for the constant heads was decreased to 1,394,600, 1,370,400, and 1,292,200 m^3 day^{-1} compared with 1,656,200 m^3 day^{-1} at base case, the well abstraction was 4,378,700 m^3 day^{-1}, the drain leakage decreased to 1,068,100, 1,027,700, and 897,500 m^3 day^{-1} compared with 1,480,900 m^3 day^{-1}. The canal leakage decreased to 6,167.40, 5,572.80, and 3,888.50 m^3 day^{-1} compared with 23,176 m^3 day^{-1}. The general heads decreased to 27,614, 26,913, and 24,522 compared with 34,346 m^3 day^{-1} at the base case.

On the other hand, the constant heads in flow were increased by 27.8, 31.2, and 43.9 for 2030, 2050, and 2070, respectively, compared to the base case. The flow to the aquifer was decreased by 19.7, 21.8, and 28.3 for 2030, 2050, and 2070, respectively, compared to the base case, while canal leakage was increased by 34.5, 38.4, and 52.3 for 2030, 2050, and 2070, respectively. The outflow to drains decreased by 27.9, 30.6, and 39.4 for 2030, 2050, and 2070, respectively, while outflow to wells remained constant where the same discharges were assigned for the model to strictly limit the discharge from the aquifer.

The total inflow/outflow decreased by 9.2%, 10.10%, and 12.90% for the years 2030, 2050, and 2070, respectively. Table 3 summarizes these percentages of increase (+)/decrease (−) of each boundary parameter for the years 2030, 2050, and 2070 compared to the current situation of the aquifer (base case).

Table 3. Percentage of difference (increase (+), or decrease (−)) for each simulation scenario (until the years 2030, 2050, and 2070) compared to the base case (current situation of the aquifer).

Boundary Parameter	% Increase (+) or Decrease (−) Compared to the Base Case		
	Until 2030	Until 2050	Until 2070
Constant heads	27.8	31.2	43.9
Flow into the aquifer	−19.7	−21.8	−28.8
Canals leakage	34.5	38.4	52.3
Total inflow	−9.2	−10.1	−12.9
Constant head	−15.8	−17.3	−22.0
Wells	0.0	0.0	0.0
Drains	−27.9	−30.6	−39.4
Canals leakage	−73.4	−76.0	−83.2
General heads	−19.6	−21.6	−28.6
Total outflow	−9.2	−10.1	−12.9

Figure 8a–c present the distribution of groundwater heads difference in the ND for the three predictive periods until the years 2030, 2050, and 2070. The results showed that increasing the ET will decrease the aquifer recharge and increase the groundwater head difference (GWHD).

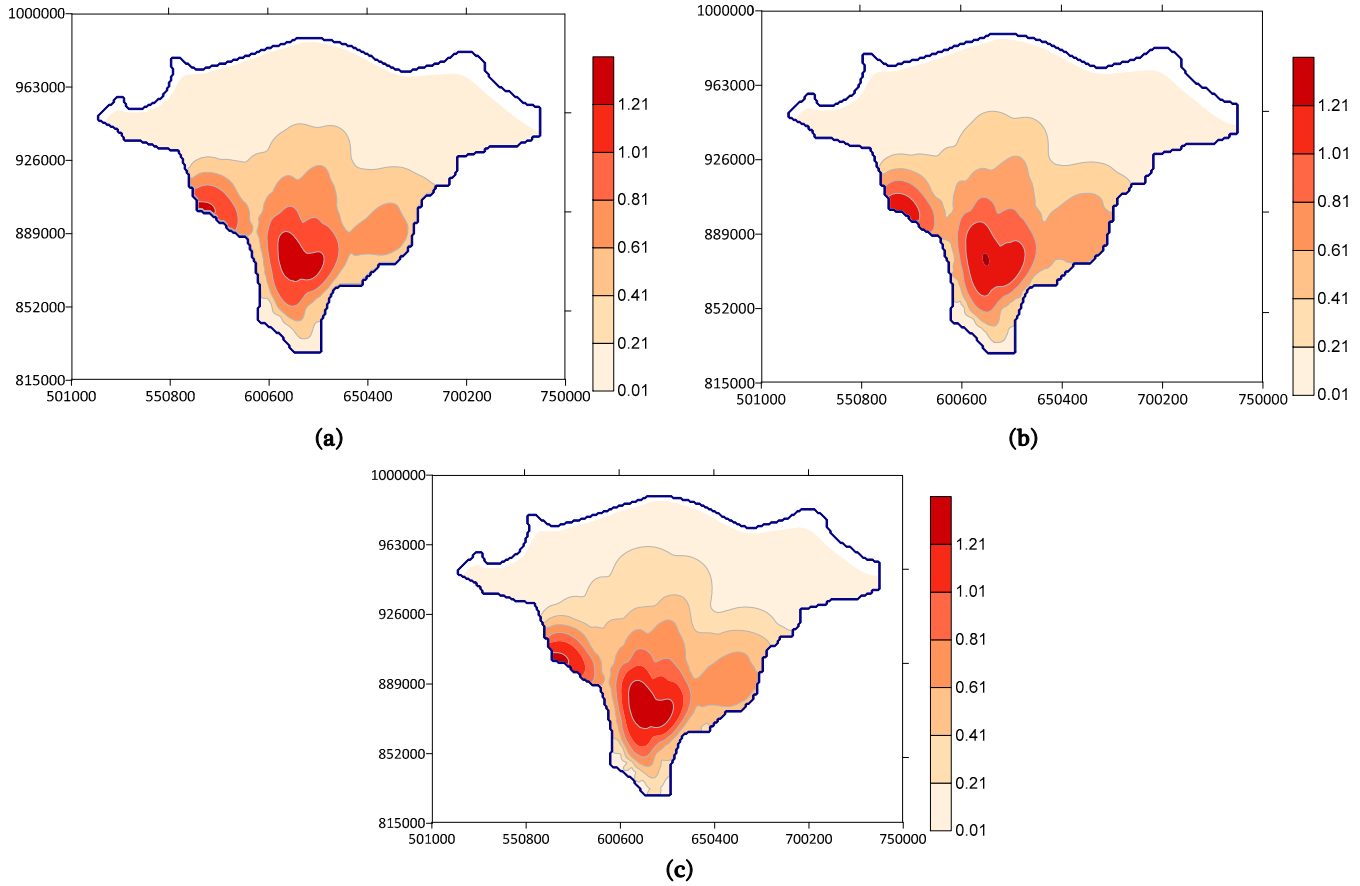

Figure 8. Distribution of groundwater head differences (in meters) for the Nile Delta aquifer for the three predictive periods: (**a**) until 2030, (**b**) until 2050, and (**c**) until 2070.

3.3. Quantification of Evapotranspiration–Aquifer Interaction

The relation between ET_c and the flow to the NDA is presented in Figure 9. The results indicated that the future increase in ET_c to 50.60 mm, 51.20 mm, and 53.70 mm year^{-1}, compared with 44.15 mm year^{-1} by an increase of 19.70%, 21.80%, and 28.80%, led to a decrease in the aquifer recharge to 4,815,900, 4,692,300, and 4,271,700 m^3 day^{-1} compared with 6,000,400 m^3 day^{-1} in the base case. The GWHD reached 0.95 m, 1.05 m, and 1.40 m while considering the increase of ET_c in years 2030, 2050, and 2070, respectively. This indicated that future ET_c should be considered in water resources management planning to mitigate the reduction of groundwater levels and any potential reduction in aquifer storage while monitoring abstraction by wells for limiting discharges from the NDA. Thus, a sustainable operation of the ND aquifer can be achieved.

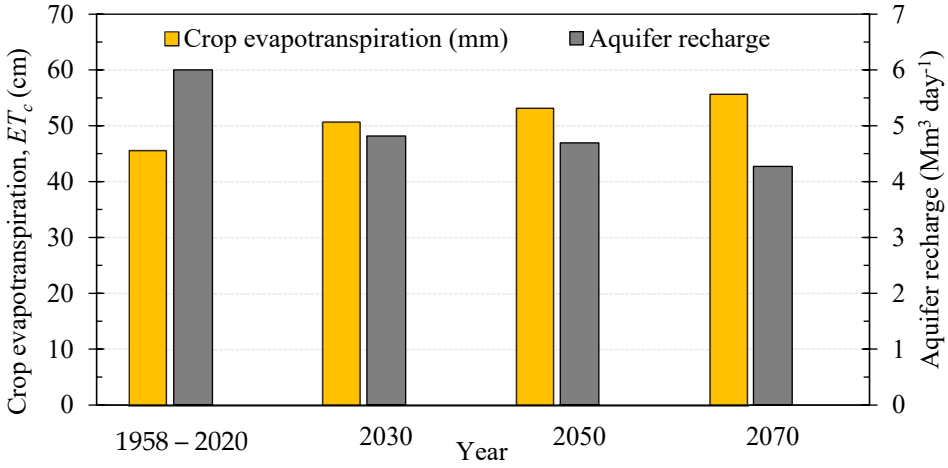

Figure 9. Comparison between the predicted average ET_c in 2030, 2050, and 2070, and the corresponding reduction in aquifer recharge (in Mm^3 day^{-1}).

4. Conclusions

Groundwater management of the Nile Delta aquifer (NDA) in Egypt was assessed by considering climate change's effect on actual evapotranspiration, ET_c (water requirements of a typical pattern). Firstly, historical data over 62 years from 1958 to 2020 were acquired, and the study area was categorized into three zones: the North (along the Mediterranean coast), the Middle, and the South. The conceptual model of MODFLOW was utilized to identify the current case of the aquifer and calculate the budget analysis after model calibration and validation in steady and transient states. Then, the visual MODFLOW was run to predict the aquifer behavior and calculate the different boundary parameters at three predictive dates: until 2030, until 2050, and until 2070, including the change of the annual actual ET_c in the North, Middle, and South zones of the Nile Delta (ND). In addition, zone budget analysis was conducted for the total inflow and outflow at the end of the three predictive periods.

Actual evapotranspiration (ET_c) in ND zones correlated with the combination of solar radiation, vapor pressure deficit, and humidity (H), which were found to be the best variables for predicting ET_c. The increasing solar radiation and vapor pressure deficit convert a considerable amount of liquid water into water vapor and water demands, while increasing humidity tends to reduce transpiration. Zone budget analysis revealed that the increase of ET_c will decrease the inflow and the outflow by 9.2, 10.1, and 12.9% in 2030, 2050, and 2070, respectively. Based on the model simulation results, the groundwater head difference (GWHD) reached 0.95, 1.05, and 1.40 m while considering the increase of ET_c in 2030, 2050, and 2070, respectively. Our results are helpful for addressing the behavior of the ND groundwater aquifer for ensuring a sustainable management plan considering the climate effect on crop water requirements. However, the combination of the spatial and temporal changes of ET_c is an interesting topic to be studied in further research.

Author Contributions: All authors whose names appear on the submission made substantial contributions. Site investigation and soil specimens were acquired and prepared for testing by M.G.E., I.A.-E., A.E., M.Z. and I.F.; numerical simulation and analysis were performed by M.G.E., I.A.-E. and I.F.; the first draft of the manuscript was written by M.G.E., I.A.-E., A.E. and I.F.; revisions and suggestions/comments on the previous versions of the manuscript were added by M.G.E., I.A.-E., A.E., M.Z. and I.F. All authors have read and agreed to the published version of the manuscript.

Funding: This work was supported by the Slovak Research and Development Agency under the Contract no. APVV-20-0281 and SK-SRB-21-0052. This work was supported by the project of the Ministry of Education of the Slovak Republic VEGA 1/0308/20 Mitigation of hydrological hazards, floods, and droughts by exploring extreme hydroclimatic phenomena in river basins.

Institutional Review Board Statement: Not applicable.

Informed Consent Statement: Not applicable.

Data Availability Statement: Data for this work can be found within the article; for further data, please contact the first and corresponding authors.

Conflicts of Interest: The authors confirm that there are no conflicts concerning the publication of this manuscript.

References

1. Loucks, D.P.; van Beek, E. Water Resources Planning and Management: An Overview. In *Water Resource Systems Planning and Management*; Springer: Cham, Switzerland, 2017. [CrossRef]
2. Abd-Elaty, I.; Saleh, O.K.; Ghanayem, H.M.; Zeleňáková, M.; Kuriqi, A. Numerical assessment of riverbank filtration using gravel back filter to improve water quality in arid regions. *Front. Earth Sci.* **2022**, *10*, 1006930. [CrossRef]
3. Genanu, M.; Alamirew, T.; Senay, G.; Gebremichael, M. Remote Sensing Based Estimation of Evapo-Transpiration Using Selected Algorithms: The Case of Wonji Shoa Sugar Cane Estate, Ethiopia. *Int. J. Sensors Sens. Netw.* **2017**, *5*, 1–13. [CrossRef]
4. Morote, A.-F.; Olcina, J.; Hernández, M. The Use of Non-Conventional Water Resources as a Means of Adaptation to Drought and Climate Change in Semi-Arid Regions: South-Eastern Spain. *Water* **2019**, *11*, 93. [CrossRef]
5. Abd-Elaty, I.; Straface, S. Mathematical Models Ensuring Freshwater of Coastal Zones in Arid and Semiarid Regions. In *Earth Systems Protection and Sustainability*; Furze, J.N., Eslamian, S., Raafat, S.M., Swing, K., Eds.; Springer: Cham, Switzerland, 2022. [CrossRef]
6. El Shinawi, A.; Kuriqi, A.; Zelenakova, M.; Vranayova, Z.; Abd-Elaty, I. Land subsidence and environmental threats in coastal aquifers under sea level rise and over-pumping stress. *J. Hydrol.* **2022**, *608*, 127607. [CrossRef]
7. Ward, F.A.; Pulido-Velazquez, M. Water conservation in irrigation can increase water use. *Proc. Natl. Acad. Sci. USA* **2008**, *105*, 18215–18220. [CrossRef]
8. Levidow, L.; Zaccaria, D.; Maia, R.; Vivas, E.; Todorovic, M.; Scardigno, A. Improving water-efficient irrigation: Prospects and difficulties of innovative practices. *Agric. Water Manag.* **2014**, *146*, 84–94. [CrossRef]
9. Abd-Elaty, I.; Kushwaha, N.; Grismer, M.E.; Elbeltagi, A.; Kuriqi, A. Cost-effective management measures for coastal aquifers affected by saltwater intrusion and climate change. *Sci. Total. Environ.* **2022**, *836*, 155656. [CrossRef]
10. Li, P.; Qian, H.; Wu, J. Conjunctive use of groundwater and surface water to reduce soil salinization in the Yinchuan Plain, North-West China. *Int. J. Water Resour. Dev.* **2018**, *34*, 337–353. [CrossRef]
11. Obaideen, K.; Yousef, B.A.; AlMallahi, M.N.; Tan, Y.C.; Mahmoud, M.; Jaber, H.; Ramadan, M. An overview of smart irrigation systems using IoT. *Energy Nexus* **2022**, *7*, 100124. [CrossRef]
12. Saggi, M.K.; Jain, S. A Survey Towards Decision Support System on Smart Irrigation Scheduling Using Machine Learning approaches. *Arch. Comput. Methods Eng.* **2022**, *29*, 4455–4478. [CrossRef]
13. Taheri, M.; Mohammadian, A.; Ganji, F.; Bigdeli, M.; Nasseri, M. Energy-Based Approaches in Estimating Actual Evapotranspiration Focusing on Land Surface Temperature: A Review of Methods, Concepts, and Challenges. *Energies* **2022**, *15*, 1264. [CrossRef]
14. Aghelpour, P.; Bahrami-Pichaghchi, H.; Karimpour, F. Estimating Daily Rice Crop Evapotranspiration in Limited Climatic Data and Utilizing the Soft Computing Algorithms MLP, RBF, GRNN, and GMDH. *Complexity* **2022**, *2022*, 4534822. [CrossRef]
15. Wanniarachchi, S.; Sarukkalige, R. A Review on Evapotranspiration Estimation in Agricultural Water Management: Past, Present, and Future. *Hydrology* **2022**, *9*, 123. [CrossRef]
16. Tasumi, M.; Allen, R.G. Satellite-based ET mapping to assess variation in ET with timing of crop development. *Agric. Water Manag.* **2007**, *88*, 54–62. [CrossRef]
17. Abd-Elaty, I.; Zelenakova, M. Saltwater intrusion management in shallow and deep coastal aquifers for high aridity regions. *J. Hydrol. Reg. Stud.* **2022**, *40*, 101026. [CrossRef]

18. Wilson, K.B.; Hanson, P.J.; Mulholland, P.J.; Baldocchi, D.D.; Wullschleger, S.D. A comparison of methods for determining forest evapotranspiration and its components: Sap-flow, soil water budget, eddy covariance and catchment water balance. *Agric. For. Meteorol.* **2001**, *106*, 153–168. [CrossRef]
19. Zhao, L.; Xia, J.; Xu, C.-Y.; Wang, Z.; Sobkowiak, L.; Long, C. Evapotranspiration estimation methods in hydrological models. *J. Geogr. Sci.* **2013**, *23*, 359–369. [CrossRef]
20. Allen, R.G.; Pereira, L.S.; Raes, D.; Smith, M. *Crop Evapotranspiration, Guidelines for Computing Crop Water Requirements*; FAO Irrigation and Drainage Paper 56; FAO: Rome, Italy, 1998; ISBN 92-5-104219-5.
21. De Caro, M.; Perico, R.; Crosta, G.B.; Frattini, P.; Volpi, G.A. Regional-scale conceptual and numerical groundwater flow model in fluvio-glacial sediments for the Milan Metropolitan area (Northern Italy). *J. Hydrol. Reg. Stud.* **2020**, *29*, 100683. [CrossRef]
22. Shah, N.; Nachabe, M.; Ross, M. Extinction Depth and Evapotranspiration from Ground Water under Selected Land Covers. *Groundwater* **2007**, *45*, 329–338. [CrossRef]
23. Doble, R.C.; Crosbie, R. Review: Current and emerging methods for catchment-scale modelling of recharge and evapotranspiration from shallow groundwater. *Hydrogeol. J.* **2017**, *25*, 3–23. [CrossRef]
24. Chen, M.; Izady, A.; Abdalla, O.A. An efficient surrogate-based simulation-optimization method for calibrating a regional MODFLOW model. *J. Hydrol.* **2017**, *544*, 591–603. [CrossRef]
25. Liou, Y.-A.; Kar, S.K. Evapotranspiration Estimation with Remote Sensing and Various Surface Energy Balance Algorithms—A Review. *Energies* **2014**, *7*, 2821–2849. [CrossRef]
26. Elkamhawy, E.; Zelenakova, M.; Abd-Elaty, I. Numerical Canal Seepage Loss Evaluation for Different Lining and Crack Techniques in Arid and Semi-Arid Regions: A Case Study of the River Nile, Egypt. *Water* **2021**, *13*, 3135. [CrossRef]
27. Rana, G.; Katerji, N. Measurement and estimation of actual evapotranspiration in the field under Mediterranean climate: A review. *Eur. J. Agron.* **2000**, *13*, 125–153. [CrossRef]
28. Xu, C.-Y.; Chen, D. Comparison of seven models for estimation of evapotranspiration and groundwater recharge using lysimeter measurement data in Germany. *Hydrol. Process.* **2005**, *19*, 3717–3734. [CrossRef]
29. Linacre, E.T. Evaporation trends. *Theor. Appl. Climatol.* **2004**, *79*, 11–21. [CrossRef]
30. Han, S.; Tian, F. A review of the complementary principle of evaporation: From the original linear relationship to generalized nonlinear functions. *Hydrol. Earth Syst. Sci.* **2020**, *24*, 2269–2285. [CrossRef]
31. Abd-Elaty, I.; Sallam, G.A.; Straface, S.; Scozzari, A. Effects of climate change on the design of subsurface drainage systems in coastal aquifers in arid/semi-arid regions: Case study of the Nile delta. *Sci. Total. Environ.* **2019**, *672*, 283–295. [CrossRef]
32. El Shinawi, A.; Zeleňáková, M.; Nosair, A.M.; Abd-Elaty, I. Geo-spatial mapping and simulation of the sea level rise influence on groundwater head and upward land subsidence at the Rosetta coastal zone, Nile Delta, Egypt. *J. King Saud Univ. Sci.* **2022**, *34*, 102145. [CrossRef]
33. Abd-Elaty, I.; Pugliese, L.; Zelenakova, M.; Mesaros, P.; El Shinawi, A. Simulation-Based Solutions Reducing Soil and Groundwater Contamination from Fertilizers in Arid and Semi-Arid Regions: Case Study the Eastern Nile Delta, Egypt. *Int. J. Environ. Res. Public Health* **2020**, *17*, 9373. [CrossRef]
34. Eltarabily, M.G. Reuse of Agriculture Drainage Water—Case Studies: Central Valley of California and the Nile Delta in Egypt. In *The Handbook of Environmental Chemistry*; Springer: Berlin/Heidelberg, Germany, 2022. [CrossRef]
35. Ashour, M.A.; Aly, T.E.; Eldegwee, Y.A. An Investigation Concerning the Impact of Climate Changes on the Water Equilibrium in the Egyptian Nile Delta. *Ann. Valahia Univ. Targoviste Geogr. Ser.* **2017**, *17*, 58–69. [CrossRef]
36. Eltarabily, M.G.; Moghazy, H.E.M. GIS-based evaluation and statistical determination of groundwater geochemistry for potential irrigation use in El Moghra, Egypt. *Environ. Monit. Assess.* **2021**, *193*, 306. [CrossRef]
37. Abd-Elaty, I.; Zelenakova, M.; Straface, S.; Vranayová, Z.; Abu-Hashim, M. Integrated Modelling for Groundwater Contamination from Polluted Streams Using New Protection Process Techniques. *Water* **2019**, *11*, 2321. [CrossRef]
38. Kambale, J.B. Impact of climate change on groundwater recharge in a semi-arid region of northern India. *Appl. Ecol. Environ. Res.* **2017**, *15*, 335–362. [CrossRef]
39. Milly, P.C.D.; Dunne, K.A. Trends in evaporation and surface cooling in the Mississippi River Basin. *Geophys. Res. Lett.* **2001**, *28*, 1219–1222. [CrossRef]
40. Golubev, V.S.; Lawrimore, J.H.; Groisman, P.Y.; Speranskaya, N.A.; Zhuravin, S.A.; Menne, M.J.; Peterson, T.C.; Malone, R.W. Evaporation changes over the contiguous United States and the former USSR: A reassessment. *Geophys. Res. Lett.* **2001**, *28*, 2665–2668. [CrossRef]
41. Mostafa, A.N.; Wheida, A.; El Nazer, M.; Adel, M.; El Leithy, L.; Siour, G.; Coman, A.; Borbon, A.; Magdy, A.W.; Omar, M.; et al. Past (1950–2017) and future (−2100) temperature and precipitation trends in Egypt. *Weather. Clim. Extrem.* **2019**, *26*, 100225. [CrossRef]
42. Yassen, A.N.; Nam, W.-H.; Hong, E.-M. Impact of climate change on reference evapotranspiration in Egypt. *Catena* **2020**, *194*, 104711. [CrossRef]
43. Ajjur, S.B.; Al-Ghamdi, S.G. Evapotranspiration and water availability response to climate change in the Middle East and North Africa. *Clim. Chang.* **2021**, *166*, 28. [CrossRef]
44. Nikiel, C.A.; Eltahir, E.A.B. Past and future trends of Egypt's water consumption and its sources. *Nat. Commun.* **2021**, *12*, 4508. [CrossRef]

45. Eltarabily, M.G.A.; Negm, A.M. Groundwater Management for Sustainable Development Plans for the Western Nile Delta. In *Groundwater in the Nile Delta*; The Handbook of Environmental Chemistry; Negm, A., Ed.; Springer: Cham, Switzerland, 2018; Volume 73. [CrossRef]
46. SNC. Egypt's Second National Communication, Egyptian Environmental Affairs Agency (EEAA-May 2010), under the United Nations Framework Convention on Climate Change on Climate Change (UNFCCC). 2010. Available online: https://unfccc.int/resource/docs/natc/egync2.pdf (accessed on 1 August 2022).
47. RIGW. *Hydrogeological Map of Nile Delta. Scale 1: 500,000*, 1st ed.; Nile Delta; Research Institute for Groundwater (RIGW), National Water Research Center (NWRC): El-Qanatir, Egypt, 1992; Internal report.
48. Abdelaty, I.M. Numerical and Experimental Study for Simulating Climatic Changes Effects on Nile Delta Aquifer. Ph.D. Thesis, Faculty of Engineering, Zagazig University, Zagazig, Egypt, 2014.
49. Elewa, H.H. Potentialities of Water Resources Pollution of the Nile River Delta. *Open Hydrol. J.* **2010**, *4*, 1–13. [CrossRef]
50. Radwan, T.M.; Blackburn, G.A.; Whyatt, J.D.; Atkinson, P.M. Dramatic Loss of Agricultural Land Due to Urban Expansion Threatens Food Security in the Nile Delta, Egypt. *Remote Sens.* **2019**, *11*, 332. [CrossRef]
51. Al-Agha, D.E.; Closas, A.; Molle, F. Survey of groundwater use in the central part of the Nile Delta. Water and Salt Management in the Nile Delta: Activity Report Number 6. 2015. Available online: https://horizon.documentation.ird.fr/exl-doc/pleins_textes/divers16-02/010066349.pdf (accessed on 1 August 2022).
52. Stanley, J.-D.; Clemente, P.L. Increased Land Subsidence and Sea-Level Rise Are Submerging Egypt's Nile Delta Coastal Margin. *GSA Today* **2017**, *27*, 4–11. [CrossRef]
53. Abd-Elaty, I.; Pugliese, L.; Bali, K.M.; Grismer, M.E.; Eltarabily, M.G. Modelling the impact of lining and covering irrigation canals on underlying groundwater stores in the Nile Delta, Egypt. *Hydrol. Process.* **2021**, *36*, e14466. [CrossRef]
54. Said, R. *The Geologic Evolution of the River Nile*; Springer: Berlin/Heidelberg, Germany, 1981.
55. Abd-Elaty, I.; Javadi, A.A.; Abd-Elhamid, H. Management of saltwater intrusion in coastal aquifers using different wells systems: A case study of the Nile Delta aquifer in Egypt. *Hydrogeol. J.* **2021**, *29*, 1767–1783. [CrossRef]
56. Ebraheem, A.-A.M.; Senosy, M.M.; Dahab, K.A. Geoelectrical and Hydrogeochemical Studies for Delineating Ground-Water Contamination Due to Salt-Water Intrusion in the Northern Part of the Nile Delta, Egypt. *Groundwater* **1997**, *35*, 216–222. [CrossRef]
57. Morsy, W.S. Environmental Management of Groundwater Resources for Nile Delta Region. Ph.D. Thesis, Faculty of Engineering, Cairo University, Cairo, Egypt, 2009.
58. Abd-Elhamid, H.F.; Abd-Elaty, I.; Negm, A.M. Control of Saltwater Intrusion in Coastal Aquifers. In *Groundwater in the Nile Delta*; Negm, A., Ed.; The Handbook of Environmental Chemistry; Springer: Cham, Switzerland, 2018; Volume 73. [CrossRef]
59. Eltarabily, M.G.; Moghazy, H.E.; Abdel-Fattah, S.; Negm, A.M. The use of numerical modeling to optimize the construction of lined sections for a regionally-significant irrigation canal in Egypt. *Environ. Earth Sci.* **2020**, *79*, 80. [CrossRef]
60. Abd-Elaty, I.; Saleh, O.K.; Ghanayem, H.M.; Grischek, T.; Zelenakova, M. Assessment of hydrological, geohydraulic and operational conditions at a riverbank filtration site at Embaba, Cairo using flow and transport modeling. *J. Hydrol. Reg. Stud.* **2021**, *37*, 100900. [CrossRef]
61. Abd-Elaty, I.; Zeleňáková, M.; Krajníková, K.; Abd-Elhamid, H. Analytical Solution of Saltwater Intrusion in Costal Aquifers Considering Climate Changes and Different Boundary Conditions. *Water* **2021**, *13*, 995. [CrossRef]
62. Mabrouk, M.; Jonoski, A.; Essink, G.O.; Uhlenbrook, S. Assessing the Fresh–Saline Groundwater Distribution in the Nile Delta Aquifer Using a 3D Variable-Density Groundwater Flow Model. *Water* **2019**, *11*, 1946. [CrossRef]
63. Abd-Elaty, I.; Shahawy, A.E.; Santoro, S.; Curcio, E.; Straface, S. Effects of groundwater abstraction and desalination brine deep injection on a coastal aquifer. *Sci. Total. Environ.* **2021**, *795*, 148928. [CrossRef]
64. Eltarabily, M.G.; Negm, A.M.; Yoshimura, C.; Saavedra, O.C. Modeling the impact of nitrate fertilizers on groundwater quality in the southern part of the Nile Delta, Egypt. *Water Supply* **2017**, *17*, 561–570. [CrossRef]
65. Smith, M. *Cropwat: A Computer Program for Irrigation Planning and Management (No. 46)*; Food & Agriculture Org.: Roma, Italy, 1992.
66. Available online: https://www.fao.org/3/V9978E/v9978e0e.htm (accessed on 1 August 2022).
67. Abatzoglou, J.T.; Dobrowski, S.; Parks, S.A.; Hegewisch, K.C. TerraClimate, a high-resolution global dataset of monthly climate and climatic water balance from 1958–2015. *Sci. Data* **2018**, *5*, 170191. [CrossRef]
68. Kobayashi, S.; Ota, Y.; Harada, Y.; Ebita, A.; Moriya, M.; Onoda, H.; Onogi, K.; Kamahori, H.; Kobayashi, C.; Endo, H.; et al. The JRA-55 Reanalysis: General Specifications and Basic Characteristics. *J. Meteorol. Soc. Jpn. Ser. II* **2015**, *93*, 5–48. [CrossRef]
69. Elbeltagi, A.; Aslam, M.R.; Mokhtar, A.; Deb, P.; Abubakar, G.A.; Kushwaha, N.; Venancio, L.P.; Malik, A.; Kumar, N.; Deng, J. Spatial and temporal variability analysis of green and blue evapotranspiration of wheat in the Egyptian Nile Delta from 1997 to 2017. *J. Hydrol.* **2021**, *594*, 125662. [CrossRef]
70. Elbeltagi, A.; Deng, J.; Wang, K.; Hong, Y. Crop Water footprint estimation and modeling using an artificial neural network approach in the Nile Delta, Egypt. *Agric. Water Manag.* **2020**, *235*, 106080. [CrossRef]
71. Elbeltagi, A.; Deng, J.; Wang, K.; Malik, A.; Maroufpoor, S. Modeling long-term dynamics of crop evapotran-spiration using deep learning in a semi-arid environment. *Agric. Water Manag.* **2020**, *241*, 106334. [CrossRef]
72. Elbeltagi, A.; Azad, N.; Arshad, A.; Mohammed, S.; Mokhtar, A.; Pande, C.; Etedali, H.R.; Bhat, S.A.; Islam, A.R.M.T.; Deng, J. Applications of Gaussian process regression for predicting blue water footprint: Case study in Ad Daqahliyah, Egypt. *Agric. Water Manag.* **2021**, *255*, 107052. [CrossRef]

73. Wang, H.F.; Anderson, M.P. *Introduction to Groundwater Modeling: Finite Difference and Finite Element Methods*; Academic Press: Cambridge, MA, USA, 1995.
74. Ghafouri-Azar, M.; Bae, D.-H.; Kang, S.-U. Trend Analysis of Long-Term Reference Evapotranspiration and Its Components over the Korean Peninsula. *Water* **2018**, *10*, 1373. [CrossRef]
75. Gocic, M.; Trajkovic, S. Analysis of trends in reference evapotranspiration data in a humid climate. *Hydrol. Sci. J.* **2014**, *59*, 165–180. [CrossRef]
76. Adeyeri, O.E.; Ishola, K.A. Variability and Trends of Actual Evapotranspiration over West Africa: The Role of Environmental Drivers. *Agric. For. Meteorol.* **2021**, *308*, 108574. [CrossRef]